

CHARGE CARRIER RECOMBINATION DYNAMICS OF SEMI CONDUCTOR PHOTOCATALYST

AN_P35 v.2; Jun. 16, Georgios Arnaoutakis¹, Massimo Cazzanelli², Zakaria El Koura², Antonio Miotello²

¹ Edinburgh Instruments Ltd, Livingston, UK

² Dipartimento di Fisica, Università di Trento, via Sommarive 14, I-38123 Povo, Trento, Italy

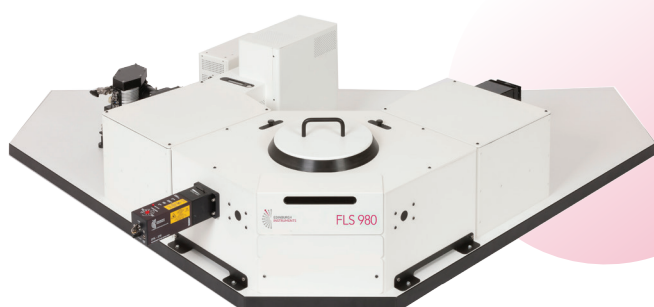


EDINBURGH
INSTRUMENTS

INTRODUCTION

Photocatalysis, the induction of chemical changes by absorption of light, is crucial for many environmental studies and sought for water splitting and hydrogen production^{1,2}, removal of pollutants^{3,4}, as well as artificial photosynthesis⁵.

With this wide spread of applications, earth-abundant photocatalysts are attracting extensive interest, especially based on anatase TiO₂ due to its abundance⁶⁻⁸ and low toxicity^{5,9}.



FLS980 Spectrometer

Due to its wide bandgap at 3.2 eV, however, it is not a good absorber in the visible range. Viable routes to extend its absorption include doping with transition metals to induce defect states in the lattice and tune the bandgap towards the visible.

In this application note, by means of time-resolved photoluminescence spectroscopy, we study the dynamics of charge carriers in copper-nitrogen-titanium oxide (Cu-N-TiO₂).

METHODS & MATERIALS

Time-resolved emission maps were performed in an FLS980 Fluorescence Spectrometer equipped with double excitation and emission monochromators, a photomultiplier tube detector (Hamamatsu, R928P) and a 450 W Xe lamp for steady-state spectral measurements. A Q-switched Nd:YAG laser (Continuum, Minilite) directly coupled to the spectrometer in L geometry was used as excitation in time-resolved measurements. The fundamental frequency of the laser was tripled, generating 355 nm light pulses of 4 ns pulse width at a repetition rate of 10 Hz and irradiance of 18 mW/cm². Gratings blazed at 400 nm were used in the excitation and emission arms, with higher diffraction orders being filtered by the integrated long wave-pass filters in the FLS980.

Thin-films of pure and Cu-N-doped TiO₂ samples were deposited on <100> silicon substrates by radio-frequency (RF) magnetron sputtering. High purity TiO₂ and copper plates were used in a vacuumed deposition chamber under argon atmosphere. For PL measurements, the samples were placed on a front face sample holder utilising 45° orientation, while a 395 nm long-pass filter placed on the sample holder was used to eliminate scattering excitation light.

RESULTS - DISCUSSION

The distinctive decay kinetics of TiO₂ and Cu-N-TiO₂ are evident in the time-resolved emission maps of Figures 1 and 2, respectively. Particularly exciton emission at 410 nm in pure TiO₂ is completely quenched in favour of the Cu-N defect states associated to the nano-columns formed at the surface of the deposited films^{10,11}.

The fit of the decays at 410 nm and 550 nm were directly extracted from the maps of Figures 1 and 2. The long-lived exciton lifetime of pure TiO₂ corresponds to a single exponent of 93 μs, displayed in Figure 3. Although the long-lived emission fits well in an equation of the form $I_{PL} = I_0 e^{-(t/\tau)}$, the recombination kinetics at 550 nm were better fit to stretched exponentials of the form $I_{PL} = I_0 e^{-(t/\tau)^\beta}$ ¹¹.

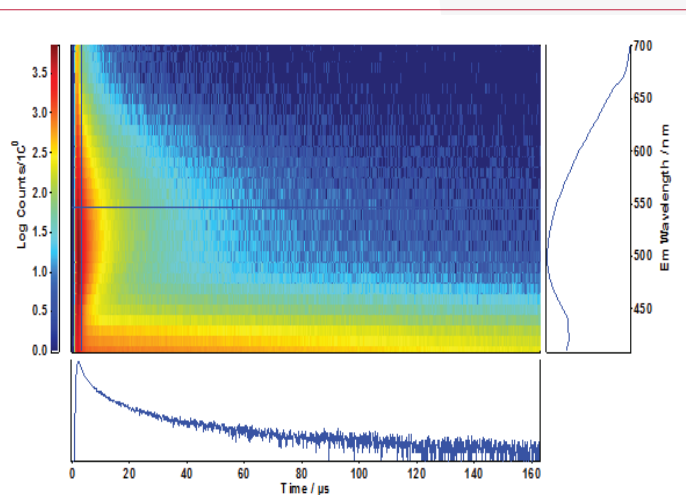


Figure 1: Time-resolved emission map of TiO₂ sample. The cross section is at 3.20 μs and 550 nm.

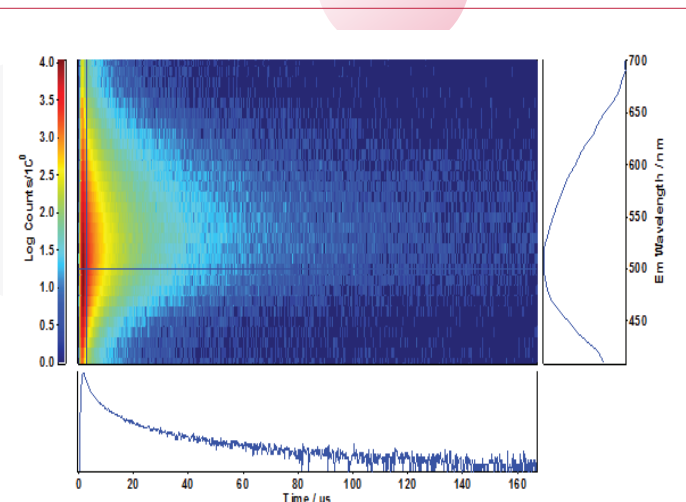


Figure 2: Time-resolved emission map of sample Cu-N-TiO₂ sample. The cross section is at 3.00 μs and 500 nm.

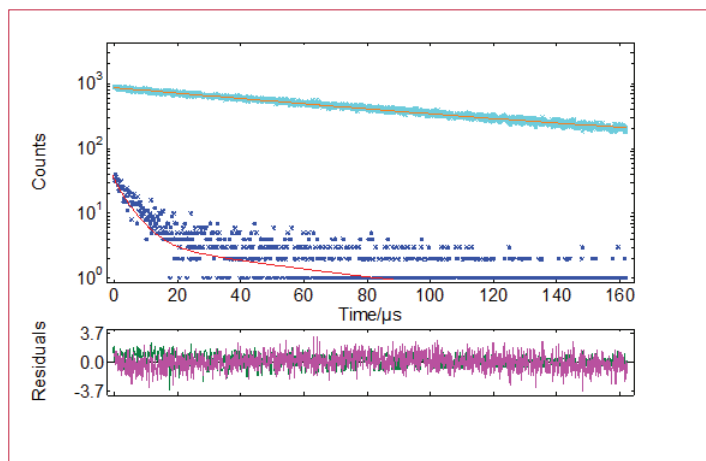


Figure 3: Photoluminescence decays of TiO_2 and Cu-N-TiO_2 samples monitored at 410 nm.

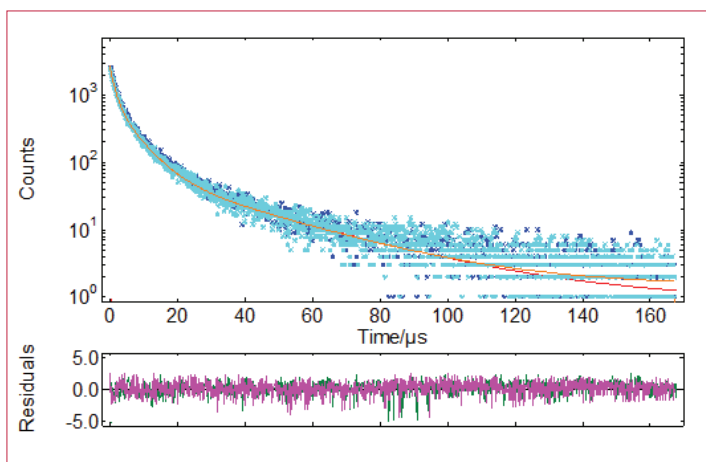


Figure 4: Photoluminescence decays of TiO_2 and Cu-N-TiO_2 samples monitored at 550 nm.

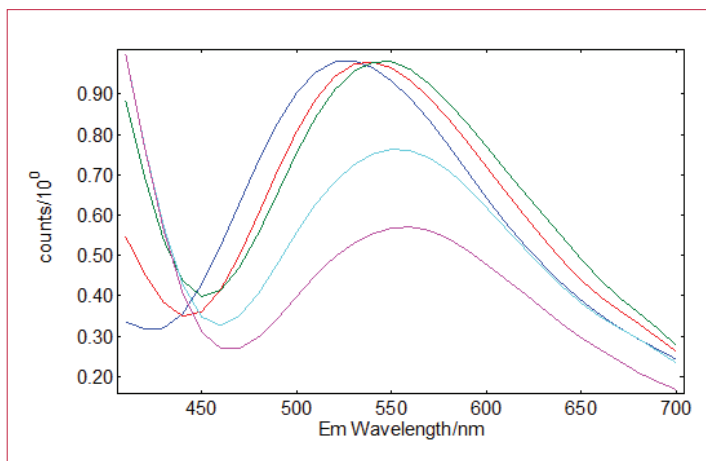


Figure 5: Time-resolved emission spectra of TiO_2 sample reconstructed from TRES maps of Figure 1.

Reported TiO_2 lifetimes vary from ns to ms depending on the preparation technique. Preparation techniques vary widely¹², with chemical vapour deposition (CVD) and RF magnetron sputtering being the most commonly used. While TiO_2 powders of 60 nm to 3 μm crystal size reported 0.04 ns - 1.3 ns¹³ and up to 2.4 ns¹⁴ lifetimes in proportion to the crystal size, anatase films grown by CVD exhibited lifetimes in the range of 10 μs - 30 μs at room temperature and 77 K^{15,16}. Similar lifetimes in the range of 10 μs - 80 μs have been reported for nanostructured semiconductors such as oxidised porous silicon¹⁰.

The time-resolved emission spectra (TRES) were readily obtained by the time-resolved emission maps in the range 32 μs - 40 μs in five bins of 2 μs width and are plot in Figures 5 and 6. It can be clearly seen that the emission of the self-trapped exciton inherent in the pure TiO_2 sample is completely quenched in the Cu-N-TiO_2 sample.

In addition to the temporal evolution of the emission spectra that can be investigated, spectra free from artefacts can also be obtained with this technique. Care needs to be taken in the acquisition of excitation and emission spectra of TiO_2 samples, weakly emitting under excitation with standard Xe lamps. As is the case of highly scattering samples such as PTFE¹⁷, experimental artefacts can be superimposed with the emission of the sample^{18,19}. This can be circumvented by the use of appropriately powered lasers as excitation sources, as demonstrated in this application note.

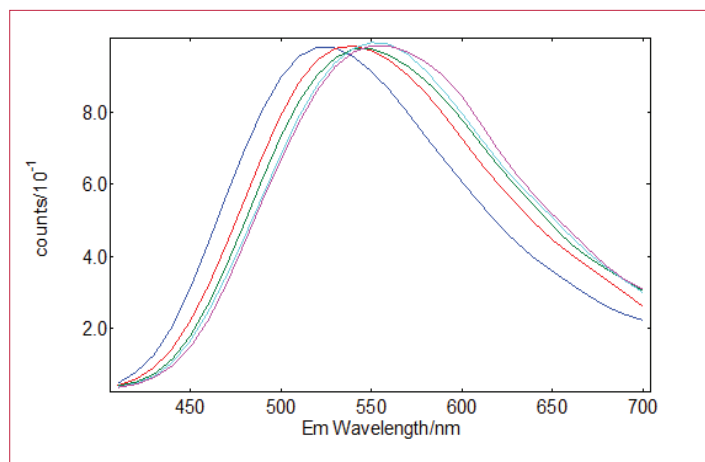


Figure 6: Normalised time-resolved emission spectra of Cu-N-TiO_2 sample reconstructed from TRES maps of Figure 2.

CONCLUSION

Charge carrier recombination in thin-films of Cu-N-TiO_2 was presented in this application note. The photoluminescence of the films was characterised by means of time-resolved spectroscopy and revealed the dynamics of charge carriers in TiO_2 by addition of Cu and N. The use of high power pulsed laser sources in conjunction with FLS980 double monochromator fluorescence spectrometers enabled this study, while minimising the manifestation of artefacts commonly evidenced for weakly emitting samples.

REFERENCES



1. Ni, M., Leung, M. K. H., Leung, D. Y. C. & Sumathy, K. A review and recent developments in photocatalytic water-splitting using for hydrogen production. *Renew. Sustain. Energy Rev.* 11, 401–425 (2007).
2. Moniz, S. J. A., Shevlin, S. A., Martin, D. J., Guo, Z.-X. & Tang, J. Visible-light driven heterojunction photocatalysts for water splitting – a critical review. *Energy Environ. Sci.* 8, 731–759 (2015).
3. Wilhelm, P. & Stephan, D. Photodegradation of rhodamine B in aqueous solution via SiO₂@TiO₂ nano-spheres. *J. Photochem. Photobiol. Chem.* 185, 19–25 (2007).
4. Ryu, J. & Choi, W. Substrate-Specific Photocatalytic Activities of TiO₂ and Multiactivity Test for Water Treatment Application. *Environ. Sci. Technol.* 42, 294–300 (2008).
5. Carp, O., Huisman, C. L. & Reller, A. Photoinduced reactivity of titanium dioxide. *Prog. Solid State Chem.* 32, 33–177 (2004).
6. Hernández-Alonso, M. D., Fresno, F., Suárez, S. & Coronado, J. M. Development of alternative photocatalysts to TiO₂: Challenges and opportunities. *Energy Environ. Sci.* 2, 1231–1257 (2009).
7. Haxel, G. B., Hedrick, J. B., Orris, G. J., Stauffer, P. H. & Hendley II, J. W. Rare earth elements: critical resources for high technology. (2002).
8. Jewell Sally & Kimball Suzette M. USGS Minerals Information: Mineral Commodity Summaries. (U.S. Department of the Interior, U.S. Geological Survey, 2016).
9. Schulz, J. et al. Distribution of sunscreens on skin. *Adv. Drug Deliv. Rev.* 54, Supplement, S157–S163 (2002).
10. Vial, J. C. et al. Mechanisms of visible-light emission from electro-oxidized porous silicon. *Phys. Rev. B* 45, 14171–14176 (1992).
11. El Koura, Z. et al. Synthesis and Characterization of Cu and N Codoped RF-Sputtered TiO₂ Films: Photoluminescence Dynamics of Charge Carriers Relevant for Water Splitting. *J. Phys. Chem. C* 120, 12042–12050 (2016).
12. Fujishima, A., Zhang, X. & Tryk, D. A. TiO₂ photocatalysis and related surface phenomena. *Surf. Sci. Rep.* 63, 515–582 (2008).
13. Fujihara, K., Izumi, S., Ohno, T. & Matsumura, M. Time-resolved photoluminescence of particulate TiO₂ photocatalysts suspended in aqueous solutions. *J. Photochem. Photobiol. Chem.* 132, 99–104 (2000).
14. Yamada, Y. & Kanemitsu, Y. Determination of electron and hole lifetimes of rutile and anatase TiO₂ single crystals. *Appl. Phys. Lett.* 101, 133907 (2012).
15. Sekiya, T., Tasaki, M., Wakabayashi, K. & Kurita, S. Relaxation process in anatase TiO₂ single crystals with different colors. *J. Lumin.* 108, 69–73 (2004).
16. Wakabayashi, K., Yamaguchi, Y., Sekiya, T. & Kurita, S. Time-resolved luminescence spectra in colorless anatase TiO₂ single crystal. *J. Lumin.* 112, 50–53 (2005).
17. Edinburgh Instruments. Comparison of Stray Light Performance for FLS980 Spectrometers with either Single or Double Monochromators. (Edinburgh Instruments).
18. Jiang, X. et al. Characterization of Oxygen Vacancy Associates within Hydrogenated TiO₂: A Positron Annihilation Study. *J. Phys. Chem. C* 116, 22619–22624 (2012).
19. Rex, R. E., Knorr, F. J. & McHale, J. L. Comment on ‘Characterization of Oxygen Vacancy Associates within Hydrogenated TiO₂: A Positron Annihilation Study’. *J. Phys. Chem. C* 117, 7949–7951 (2013).

For more information, contact:

Edinburgh Instruments

2 Bain Square,
Kirkton Campus,
Livingston, EH54 7DQ
United Kingdom.

T: +44 (0)1506 425 300

F: +44 (0)1506 425 320

E: sales@edinst.com

W: www.edinst.com